Optical molecular imaging: Luker and Luker provide an overview of current optical imaging technologies for preclinical and clinical applications and highlight the potential of these techniques in advancing molecular medicine. . . . . ***Page 1***

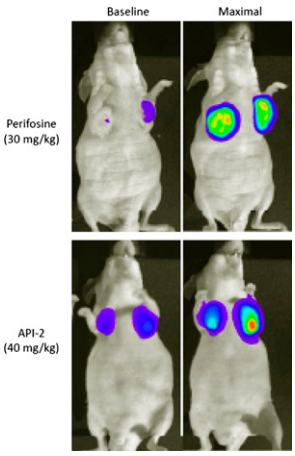

V/Q scans remain valuable: Freeman compares the advantages of traditional ventilation-perfusion scintigraphy and the rapidly increasing use of multidetector CT angiography in the detection of pulmonary embolic disease, with special reference to radiation exposure. . . . ***Page 5***

Weighing posttherapy PET benefits: Juweid reviews supporting evidence and recent international recommendations for routine use of ^{18}F-FDG PET for posttreatment assessment of patients with Hodgkin's disease and diffuse large B-cell lymphoma. . . . . ***Page 9***

PET and lymphoma response: Terasawa and colleagues report on a systematic metaanalysis of the utility of ^{18}F-FDG in detecting residual disease after first-line therapy for Hodgkin's disease and aggressive non-Hodgkin's lymphoma. . . .***Page 13***

Complementary PET tracers: Beer and colleagues describe investigations to determine the extent and nature of correlation between ^{18}F-galacto-RGD and ^{18}F-FDG PET assessments of $\alpha_v\beta_3$ expression and glucose metabolism, respectively, in cancer patients. . . . . ***Page 22***

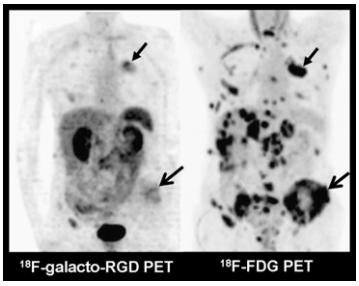

α-Particle radioimmunotherapy: Zalutsky and colleagues explore the feasibility of regionally targeted, postresection radiotherapy with a ^{211}At-labeled monoclonal antibody in patients with recurrent malignant brain tumors. . . . . ***Page 30***

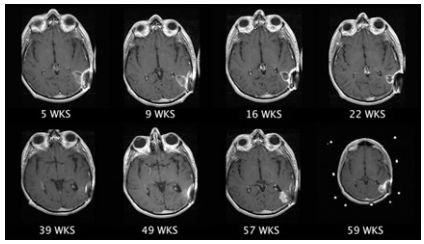

Probabilistic MCA atlas: Kim and colleagues describe a population-based technique for the use of SPECT in generating probabilistic maps of blood flow distribution in the middle cerebral artery. . . . . ***Page 39***

Mapping cortical glucose consumption: Klein and colleagues investigate the applicability of cortical flattening of MR images coregistered to high-resolution research tomographic ^{18}F-FDG PET. . . . . ***Page 44***

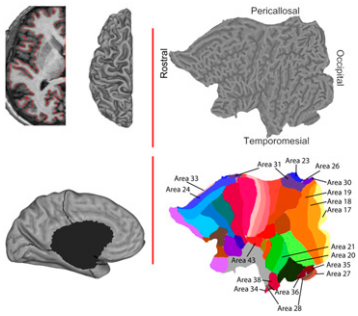

Resolving 3D ^{15}O brain PET: Ibaraki and colleagues compare 3D quantitative ^{15}O PET with 2D PET in assessment of brain pathophysiology and discuss optimal means for scatter correction. . . . ***Page 50***

PET and cochlear implants: Coez and colleagues analyze cochlear implant activation of human temporal voice areas using a standardized $H_2{}^{15}O$ PET paradigm adapted from previous functional MR imaging studies. . . . . ***Page 60***

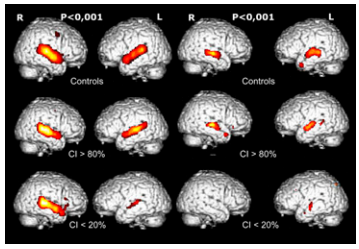

^{18}F-fluoride bone scans: Grant and colleagues provide an educational overview of ^{18}F-fluoride PET in skeletal imaging, including production, pharmacology, dosimetry, clinical applications in both benign and malignant disease, and practical and technical issues. . . . . ***Page 68***

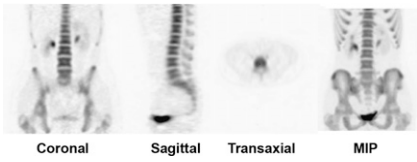

High-resolution PET insert: Wu and colleagues detail the development of a prototype system to evaluate an insert device designed to achieve higher resolution with an existing general-purpose animal PET scanner. . . . . ***Page 79***

Small-animal SPECT/MRI: Goetz and colleagues report on the development of a pinhole SPECT/low-field MRI hybrid system with potential as a low-cost solution for anatomic and functional preclinical molecular imaging. . . . . ***Page 88***

In vivo islet cell SPECT: Tai and colleagues visualize both reporter gene expression in and location of transplanted pancreatic cells in living mice using dual-isotope SPECT, a technique with promise in monitoring innovative treatments for diabetes. . . . . ***Page 94***

^{64}Cu-Nanoparticle lung imaging: Rossin and colleagues evaluate the use of PET to image lung uptake and distribution of radiolabeled and antibody-coated fluorescent nanoparticles and discuss the potential for this approach in preclinical screening of novel drug delivery agents. . . ***Page 103***

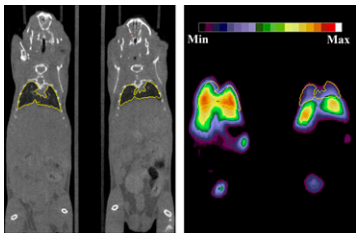

Receptor imaging in prostate cancer: Zhang and colleagues describe the development of a probe specific for a ^{64}Cu-labeled VPAC1 receptor and initial PET imaging of experimental and spontaneous human prostate cancers in mice. . . ***Page 112***

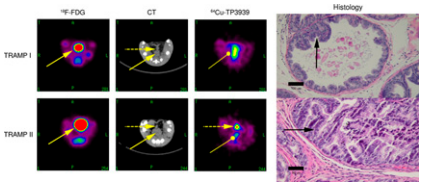

^{99m}Tc-GSA imaging in liver regeneration: de Graaf and colleagues report on ^{99m}Tc-DTPA-galactosyl serum albumin scintigraphy combined with SPECT for the assessment of liver function and liver functional volume in normal and regenerating rat livers. . . . . ***Page 122***

microPET imaging of c-Met antibody: Tseng and colleagues use small animal ^{18}F-FDG PET to investigate the efficacy of a novel antineoplastic chemotherapeutic agent and discuss the potential of this approach in assessing early response to therapy. . . . . ***Page 129***

^{11}C-Methionine PET in tumor differentiation: Zhao and colleagues detail the respective potentials of ^{18}F-FLT and ^{11}C-methionine PET in differentiating malignant tumors from granulomas and compare these capabilities with those of ^{18}F-FDG PET. . . . . ***Page 135***

Destabilized HSV1-TK reporter systems: Hsieh and colleagues describe the creation of a transcription reporter and molecular probe that allow for dynamic studies of short-time-scale gene expression events. . . . . ***Page 142***

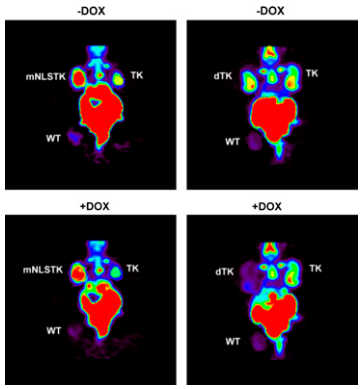

Electron dose distribution: Champion and colleagues introduce a Monte Carlo code for assessing electron dose for isolated ^{131}I in spheres of various sizes, provide representative S values, and discuss the potential for evaluating electron map deposits for any isotope. . . . . ***Page 151***

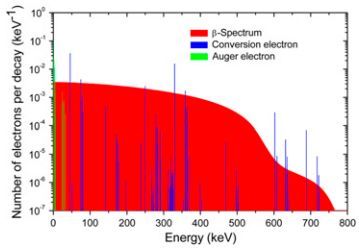

Pretargeting with bispecific antibodies: Goldenberg and colleagues report on the "Dock-and-Lock" method, a new approach to developing bioactive targeting molecules with multivalency and multifunctionality for improved cancer imaging and therapy. . . . . ***Page 158***

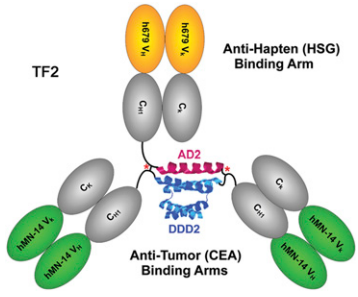

ON THE COVER

In small-animal SPECT, regions of increased radiotracer uptake are more easily localized through coregistration with anatomic images of the same animal. Here, low-field-strength MR images of the 3 orthogonal planes are coregistered with pinhole ^{99m}Tc-DMSA SPECT images. The matching of the kidneys between the functional and the anatomic images demonstrates the practical advantage of this dual-modality system.

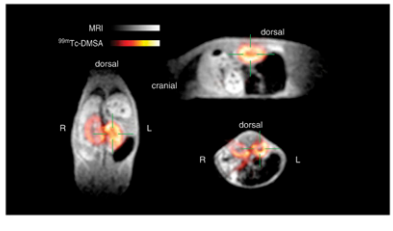

See page 91.